SURFACE ELEVATION IN A DIRECTIONALLY SPREAD WAVE GROUP AROUND A CYLINDER

E. V. Buldakov, P. H. Taylor and R. Eatock Taylor[1]

Department of Engineering Science, University of Oxford, Parks Road, Oxford OX1 3PJ, UK

SUMMARY

The problem of diffraction of a directionally spread focused incoming wave group by a bottom-seated circular cylinder is considered from the view point of second-order perturbation theory. It is shown that in the far-field such an incoming wave can be represented as a cylindrical wave-front with directionally modulated amplitude. After applying the time Fourier transform and separation of the vertical variable the resulting two-dimensional non-homogeneous Helmholtz equations are solved numerically by using finite differences. The detailed formulation of the second-order radiation condition is presented. The numerical solutions of the problem are obtained for Gaussian spreading functions of various bandwidths and various amplitude spectra including Gaussian and Pierson-Moskovitz. It is shown that the same complex structure of the local second-order elevation near the body takes place for both unidirectional and spread cases, and the amplitude of the surface elevation around the cylinder for a directionally spread wave is smaller than that for a unidirectional one.

1 PROBLEM FORMULATION

The solution of the diffraction problem depends on the following set of dimensional parameters: radius of the diffracting cylinder $\tilde{a}$; maximal amplitude of the incoming wave group $\tilde{A}$; uniform water depth $\tilde{h}$ and gravity acceleration $\tilde{g}$. After the introducion of non-dimensional coordinates $(\tilde{x}, \tilde{y}, \tilde{z}) = \tilde{a}\,(x, y, z)$; $\tilde{\Xi} = \tilde{A}\,\Xi$; $\tilde{t} = \sqrt{\tilde{a}/\tilde{g}}\,t$; $\tilde{\Phi} = \tilde{A}\,\sqrt{\tilde{a}\,\tilde{g}}\,\Phi$ the non-linear formulation includes the explicit amplitude parameter $\varepsilon = \tilde{A}/\tilde{a}$, which is the measure of non-linearity of the problem. We consider the limit $\varepsilon \to 0$ and take into account two first terms of the corresponding asymptotic expansion. Applying the time Fourier transform to the first-order homogeneous and second-order non-homogeneous problems we arrive at the following formulation for the Fourier transforms of the velocity potential ϕ and surface elevation ξ

$$\Delta\phi^{(1,2)} = 0; \qquad \frac{\partial\phi^{(1,2)}}{\partial z} = 0\,\Big|_{z=-h}; \quad \frac{\partial\phi^{(1,2)}}{\partial r} = 0\Big|_{r=1};$$
$$-\omega^2\,\phi^{(1,2)} + \frac{\partial\phi^{(1,2)}}{\partial z} = rhs^{(1,2)}\,\Big|_{z=0}; \quad \xi^{(1,2)} = i\,\omega\,\phi^{(1,2)} + se^{(1,2)}\,\Big|_{z=0},$$

where $rhs^{(1)} = 0$; $\quad se^{(1)} = 0$; $\quad rhs^{(2)} = rhs^{+} + rhs^{-}$; $\quad se^{(2)} = se^{+} + se^{-}$. The convolution integrals of the right hand side $rhs^{(2)}$ and the quadratic part of the surface elevation $se^{(2)}$, arising after applying the Fourier transform to the quadratic non-linearities, are represented as sums of plus and minus terms corresponding to the sums and differences of the various first-order frequency components respectively.

Next, we separate the vertical variable, representing each frequency component of the velocity potential as a Fourier series with eigen functions in the z-direction. Each vertical Fourier component satisfies the two-dimensional Helmholtz equation in the (x, y)-plane

$$\Delta\psi_m \pm k_0^2\,\psi_m + rhs^{(2)}(x, y) = 0 \tag{1}$$

with a no-flow condition on the cylinder and an appropriate radiation condition at infinity. A plus sign should be taken for $m = 0$ and a minus sign otherwise. More details of the problem formulation can be found in [1], which deals with the unidirectional case.

2 INCOMING WAVE

The particular solution of the diffraction problem for a prescribed geometry is completely specified by the flow behaviour at infinity, i.e. by the incoming wave. For the second-order problem it is sufficient to specify the first-order incoming wave, which in the general case can be described as a superposition of monochromatic travelling waves of different frequencies approaching the diffracting body from different directions

$$\Xi_I^{(1)}(r, \theta, t) = \frac{1}{2}\int_{-\pi}^{\pi} d\alpha \int_{-\infty}^{+\infty} DS(\Omega, \alpha)\,e^{i\,(\,k(\Omega)\,r\cos(\theta-\alpha) - \Omega\,t + \varphi(\Omega)\,)}\,d\Omega. \tag{2}$$

In this paper we separate directional and frequency parts of the general spectrum and represent it in the form $DS(\theta, \omega) = D(\theta)S(\omega)$, assuming that the spreading is the same for all frequency components. We use a simple Gaussian directional spreading function

$$D(\theta) = \frac{1}{\delta\sqrt{\pi}}\,e^{-\theta^2/\delta^2}$$

[1]Corresponding author: R.EatockTaylor@eng.ox.ac.uk

with various bandwidths δ to describe waves generated at minus infinity ($\theta = \pi$) and propagating in the positive x-direction. As δ tends to zero $D(\theta)$ approaches a δ-function corresponding to a unidirectional incoming wave. Gaussian and Pierson-Moskovitz spectra are used as amplitude spectra of the incoming wave group $S(\omega)$. Two important features of the individual frequency components from (2),

$$\xi_I(\omega) = \frac{1}{2} \int_{-\pi}^{\pi} D(\alpha) e^{i\, k(\omega)\, r \cos(\theta - \alpha)}\, d\alpha, \tag{3}$$

should be noted. For a monochromatic directionally focused wave (3) with a Gaussian spreading function the size of the focus spot can be estimated as $r_f \sim 1/(k(\omega)\,\delta)$. The focus radius is an essential characteristic of a directionally spread wave. Inside the focus spot the amplitude of such a wave is almost constant and the wave is almost unidirectional. Thus, if the diffracting body is placed inside the focus spot then the diffracted field is almost the same as one for the unidirectional wave of the same amplitude. Furthermore, using the stationary phase method it can be shown that for large r equation (3) has the following asymptotic behaviour

$$\xi_I(\omega) \to \frac{1}{2} \frac{\sqrt{\pi}}{\sqrt{k(\omega)}} (\, 1 \mp i\,)\, D(\theta - \frac{\pi}{2} \pm \frac{\pi}{2}) \frac{1}{\sqrt{r}} e^{\pm i k(\omega) r} \quad \text{as} \quad r \to \infty, \tag{4}$$

where the upper sign is taken when $x > 0$ and the lower one otherwise. This means that in the far-field the directionally focused wave can be represented in terms of the geometrical optics approximation as a cylindrical wavefront, with appropriately directed wave vector and amplitude increasing toward the centre of the front with the square root of radius.

3 NUMERICAL APPROACH

The two-dimensional Helmholtz equations (1) obtained after separation of the vertical variable for each vertical Fourier component are solved directly by using finite differences. One of the reasons for choosing this approach is that it can be easily generalised for the case of a non-circular cylinder. Based on the cylindrical far field structure of the incoming wave (4) as well as the similar behaviour of the radiated field and the diffracting body geometry, cylindrical coordinates are appropriate for this problem. The set of boundary value problems for various m was solved for every frequency component with automatic choice of the size of the computational domain and number of grid nodes in the radial direction for each frequency. Due to difficulties arising in formulation of the boundary condition at the outer boundary of the computational domain it was found convenient to separate the incoming and diffracted waves and solve the corresponding problems separately.

Let us now consider the details of the numerical procedure for obtaining solutions for individual second-order frequency components. Note that the frequency sets where such solutions are calculated are different for plus and minus terms. As a first step we calculate the convolution integrals of the right hand sides at each node of the cylindrical computational grid by using the first-order analytical solutions. After this, equations (1) written in cylindrical coordinates with proper boundary conditions are approximated by finite differences on a uniform rectangular grid in the (r,θ)-domain: $r \in [r_{\min}; r_{\max}]$, $\theta \in [0; \pi]$, where $r_{\min} = 1$ for the diffracted and $r_{\min} = 0$ for the incoming components. A symmetry condition $\partial\psi/\partial\theta = 0$ is used on the central axis $\theta = \pi$, $\theta = 0$. The resulting discrete linear algebraic equations are solved by direct method by using LU-decomposition.

One must be careful in specifying the boundary conditions for (1) especially the outer boundary condition for the case $m = 0$, when numerical generation of non-physical free waves approaching the cylinder from outside of the computational domain is possible. There are two types of outer condition: a Sommerfeld radiation condition for a free wave; and a far-field asymptotic condition for the non-homogeneous term of the solution corresponding to the locked wave. The former has the form $\psi_F \to \psi_{Fa}(r,\theta) = C(\theta) e^{ikr}/\sqrt{r}$ for $m = 0$ and decays exponentially for $m > 0$. The latter depends on the particular form of the far-field behaviour of the right hand side. It can be shown that the plus term of the locked components at large r behaves like

$$\psi_L^+ \to \psi_{La}^+(r,\theta) = \frac{1}{r^{3/2}} (\, A_0(\theta) + \frac{1}{r} A_1(\theta) + \frac{1}{r^2} A_2(\theta) + \cdots)\, e^{2ikr} \quad \text{as} \quad r \to \infty, \tag{5}$$

where the coefficients can be expressed analytically through the coefficients of the similar asymptotic expression of the right hand side. We calculate the coefficients of the 3-term right hand side far-field asymptotics from the actual right hand side using the least squares method. Now we can specify the boundary conditions on the outer boundary of the computational domain $r = r_{\max}$ for the plus diffracted component as follows:

$$\psi_D^+(r_{\max},\theta) = \psi_{La}^+(r_{\max},\theta) + \psi_{Fa}(r_{\max},\theta); \quad \frac{\partial}{\partial r}\psi_D^+(r_{\max},\theta) = \frac{\partial}{\partial r} \left(\psi_{La}^+(r_{\max},\theta) + \psi_{Fa}(r_{\max},\theta)\right).$$

The second condition is used for $m = 0$ to calculate unknown *a priori* values of a coefficient of the free wave asymptotics $C(\theta)$ at each node of the outer boundary. For $m > 0$ there is no free radiated component and we can take $C(\theta) = 0$. The second-order incoming wave consists only of locked components and the sum term has

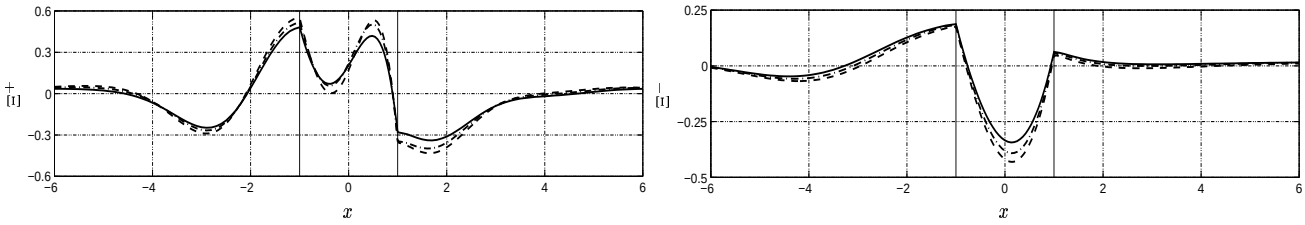

Figure 1: Second order plus (left) and minus (right) surface elevation for various bandwidth of the Gaussian spreading function: ——— – $\delta = 0.5$; – · – · – – $\delta = 0.3$; – – – – unidirectional. Gaussian amplitude spectrum of the incoming wave group, $\omega_0 = 0.680$, $\Delta = 0.21$, $h = 10.43$.

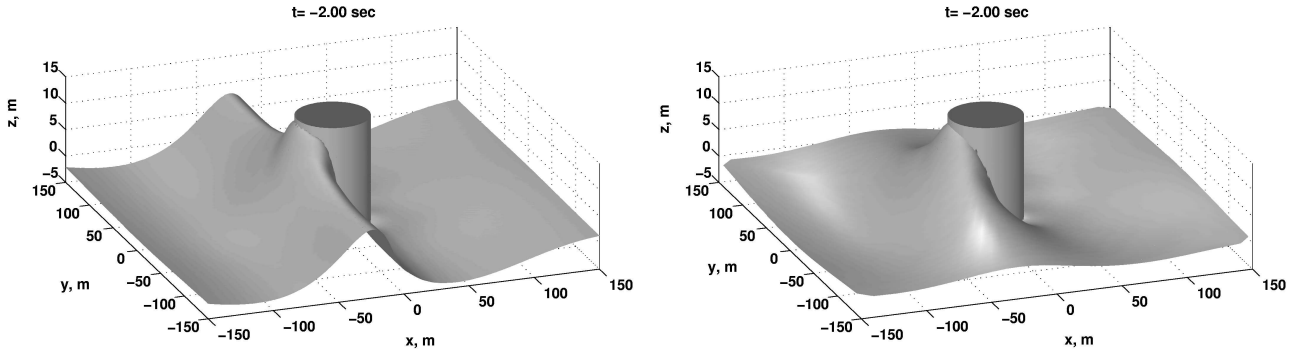

Figure 2: The total surface elevation around the cylinder for the Pierson-Moskovitz amplitude spectrum of the incoming wave group. Unidirectional incoming wave (left) and directionally spread incoming wave (right) with bandwidth of the Gaussian spreading function $\delta = 0.5$.

the same far-field behaviour as the radiated locked wave (5) for $x > 0$ (outgoing wave). The incoming part ($x < 0$) has similar behaviour, with the wave vector in the opposite direction. The appropriate outer boundary condition for the plus term of the incoming wave includes the specification of the asymptotic behaviour for the upstream solution and free propagation of the outgoing wave downstream of the cylinder, which according to the first term of (5) has the form

$$r^{3/2}\left(\frac{\partial}{\partial r}\psi - 2ki\,\psi\right) \to 0 \quad \text{as} \quad r \to \infty.$$

At the centre of the grid $r = 0$ the value of the potential should be the same for every mesh point. It is also essential to ensure the absence of a point wave source in the centre of the grid, which leads to an additional condition at $r = 0$:

$$\oint \frac{\partial \psi}{\partial r}\, d\theta = 0.$$

For the minus term we do not know the exact form of far field behaviour for the locked term, but we can use the fact that the solution has an exponentially decaying asymptotic behaviour similar to that of the precalculated minus term of the right hand side. Otherwise the formulation of the boundary conditions is similar to the plus term.

4 RESULTS

The numerical solution of the problem was obtained for various amplitude spectra of the incoming wave and various bandwidths δ of the Gaussian spreading function. Examples of the results obtained during these calculations are presented in figures 1-3. Figure 1 shows the comparison of second-order plus and minus surface elevations for cases with different directional spreading δ. The incoming wave group has a Gaussian frequency spectrum with the following non-dimensional parameters: peak frequency $\omega_0 = 0.680$, bandwidth $\Delta = 0.21$, depth $h = 10.43$. The wave is focused on the cylinder axis. The result for the unidirectional case was obtained by the method described in [1]. It can be seen that for decreasing bandwidth of directional spreading the solutions approach that for the unidirectional incoming wave. As the incoming wave has a relatively low frequency, the size of the focus spot is rather large and the difference between the cases presented in figure 1 is small.

Next, we apply the method to the case of an incoming wave group with the Pierson-Moskovitz amplitude spectrum with physical parameters: amplitude $\tilde{A} = 8.15\,\mathrm{m}$, depth $\tilde{h} = 50\,\mathrm{m}$, cylinder radius $\tilde{a} = 25\,\mathrm{m}$ and characteristic period of the wave $\tilde{T}_0 = 12\,\mathrm{sec}$. The corresponding non-dimensional parameters are $h = 2$,

$\omega_0 = 0.836$ and $\varepsilon = 0.326$. Figure 2 shows the complete first plus second-order surface elevations around the cylinder for the unidirectional incoming group and for a spread group in which the bandwidth of the Gaussian spreading function $\delta = 0.5$, at the time when the elevation at the front stagnation point is close to maximal. The difference between the unidirectional and spread cases seen in figure 2 is mostly due to the incoming wave. This also leads to the difference in the second-order locked diffracted component. Nevertheless, the behaviour of the incoming waves near the circumference of the cylinder is similar for both cases because the size of the focus spot is comparable to a cylinder radius. The first-order diffracted wave as well as the second-order free diffracted components are generated in the process of interaction of the incoming wave with the surface of the diffracting object, and are completely specified by the behaviour of the incoming wave around the circumference of the cylinder. Thus we can expect that the free diffracted components will exhibit similar behaviour for both cases. Moreover, the amplitude of the directionally spread incoming wave near the surface of the cylinder is smaller than that for the unidirectional case, because it decreases in the transverse direction. Hence the amplitude of the free radiated waves for the spread case should be smaller than for the unidirectional one. The results of the calculations show that this is actually the case. In figure 3 contour plots of the second-order plus-elevation for both unidirectional and spread incoming waves are represented. The difference between the locked component of the plus-term of the incoming wave can be seen in the figure. The second order free radiated waves are generated in the process of interaction of the incoming wave with the surface of the cylinder, which can be clearly detected on the last three snapshots. The same complex structure of the local second-order surface field near the body arises in both cases; however the amplitude is smaller for the case of the directionally spread waves.

This work was supported by the Engineering and Physical Science Research Council, grant GR/M 98814.

[1] Buldakov, E. V., Taylor, P. H. & Eatock Taylor, R. 2002 Second order diffraction of a unidirectional wave group. In *Proc. 17th Int. Workshop on Water Waves and Floating Bodies*, pp. 17–20. Cambridge, UK.

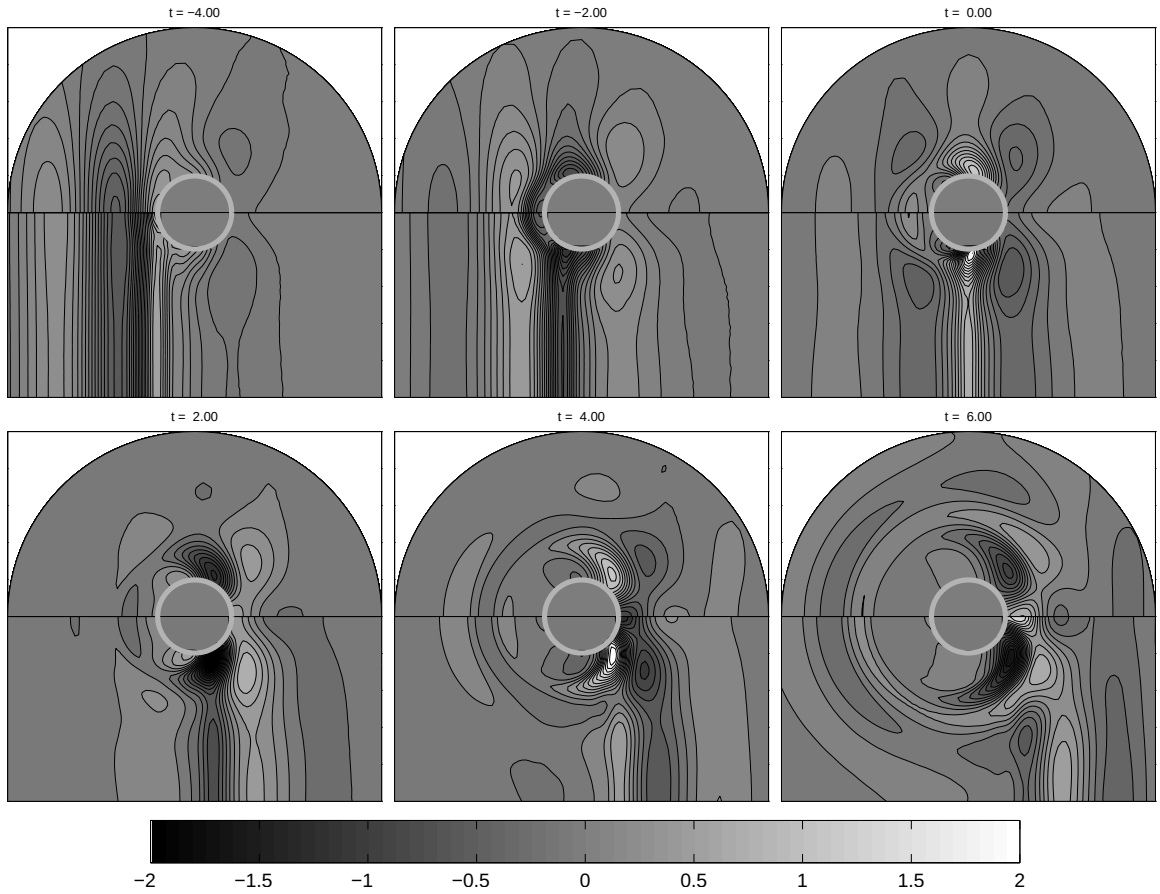

Figure 3: Contour plots of the second-order plus term Ξ^+ of surface elevation for unidirectional (lower part) and spread (upper part) wave groups for various time moments.

Question by : T. Miloh
It is known that the second order solution for the classical Neumann-Kelvin solution of the diffraction of a monochromatic wave by a vertical cylinder has a logarithmic solution at the confluence of the free surface and cylinder. Did you encounter similar type of singularity in your study of wave groups?

Author's reply:
This singularity takes place in the solution for a locked wave. When we construct the solution numerically, we include both locked and free components and the singularity is cancelled out by adding the free component with the opposite singularity in the process of satisfaction of boundary conditions. When we performed calculations with only locked components for testing purposes, this singularity was observed.
